Effect of annealing time and temperature on the formation of threading and projected range dislocations in 1 MeV boron implanted Si

K. S. Jones
Department of Materials Science and Engineering, SWAMP Center, University of Florida, Gainesville, Florida 32611

Craig Jasper
Motorola, Predictive Engineering Laboratory, 2200 West Broadway Road, Mesa, Arizona 85202

Allen Hoover
ON Semiconductors, 2200 West Broadway Road, Mesa, Arizona 85202

(Received 18 August 2000; accepted for publication 12 January 2001)

The effect of annealing temperature and time on the formation of threading dislocations was investigated for high energy boron implants into silicon. 1 MeV B^+ was implanted at a dose of $1\times10^{14}/cm^2$ into $\langle100\rangle$ Si wafers. The wafers were subsequently annealed in either a rapid thermal annealing (RTA) furnace or a conventional furnace for times between 1 s and 1 h at temperatures between 700 and 1150 °C. Following this anneal the wafers were put through a standard complementary metal-oxide-semiconductor (CMOS) process. After processing, the threading dislocation density and projected range dislocation density were studied using etch pit density counts and transmission electron microscopy (TEM). The results show that annealing (either RTA or furnace) at temperatures above 1000 °C prior to CMOS processing reduced the high density of threading dislocations by 1–2 orders of magnitude. Quantitative plan-view TEM studies show that the mechanism for defect reduction is different for the RTA versus furnace annealing and may be ramp rate dependent. © *2001 American Institute of Physics.* [DOI: 10.1063/1.1355006]

The use of high energy implantation has been shown to be very promising for a variety of Si processing steps including the formation of buried doping wells and gettering layers.[1–5] Commonly the doses used for both boron and phosphorus are below the amorphization threshold but are sufficient to result in dislocation loop formation near the projected range of the implant upon subsequent annealing.[6–10] It has been observed that often a fraction of these dislocation loops intersect the surface resulting in the formation of threading dislocations.[11] These threading dislocations can have adverse effects on the gate oxide integrity and leakage currents.[12] There have been several studies investigating the dependence of these threading dislocations on implant dose, energy species, and starting wafer.[11,13–16] It has also been observed in these studies, that as a function of boron implant dose the threading dislocation density exhibits a maximum at a dose of around $1\times10^{14}/cm^2$. The purpose of this study is to investigate the effect of annealing temperature and time on the evolution of the threading dislocation density at this critical dose of $1\times10^{14}/cm^2$.

The high energy boron implants were carried out in 7-μm-thick lightly doped ($1\times10^{15}/cm^3$) p-type epitaxial silicon grown on $\langle100\rangle p^+$ silicon. A single boron implant at a dose of $1\times10^{14}/cm^2$ at 1 MeV was performed. Selected samples were annealed in a rapid thermal annealing (RTA) furnace at a ramp rate of 50 °C/s at varying times and temperatures. Likewise, other samples were annealed in a conventional furnace for 30 min at a ramp rate of 10 °C/s for varying temperatures. Upon completion of the initial anneal all the samples were annealed in a conventional furnace at 800 °C for 90 min followed by a 550 °C anneal for 60 min and finally a 950 °C anneal for 10 min.

For the etch pit studies, after annealing a piece of each wafer was etched using a Schimmel[17] etch for 30 s. Dark field optical microscopy was used to quantify the etch pit density. Bourdelle *et al.*[16] have shown recently that there is a good correlation between the etch pit density and the threading dislocation density, although a few dislocations may not be etched. The etching process allowed for quantification of defect densities between 1×10^4 and $1\times10^7/cm^2$. Plan-view transmission electron microscopy (TEM) was used to characterize the defect density at the projected range. Because the projected range of the B implants was approximately 1.7 μm and the TEM at 200 kV has difficulty discerning defects >1 μm deep, it was necessary to use a cylindrical molecular pump to remove approximately 1.2 μm of the surface prior to TEM sample preparation. The amount removed was calibrated by cross-sectional TEM. Standard backside etching was used for the plan-view sample preparation. TEM examination was done on a JEOL 200CX using a $\mathbf{g}_{220}$ bright field imaging condition.

Figure 1 shows bright field images of the dependence of the dislocation density at the projected range on the annealing temperature for both 30 s RTA anneals and 60 min furnace anneals. It is clear there is a marked difference between the two processes. For the RTA samples increasing the temperature increases the density of the projected range loops but decreases their size. For the furnace annealed samples, the defect density decreases rapidly with increasing temperature. These observations are summarized quantitatively in Fig. 2. This graph shows how the threading dislocation den-

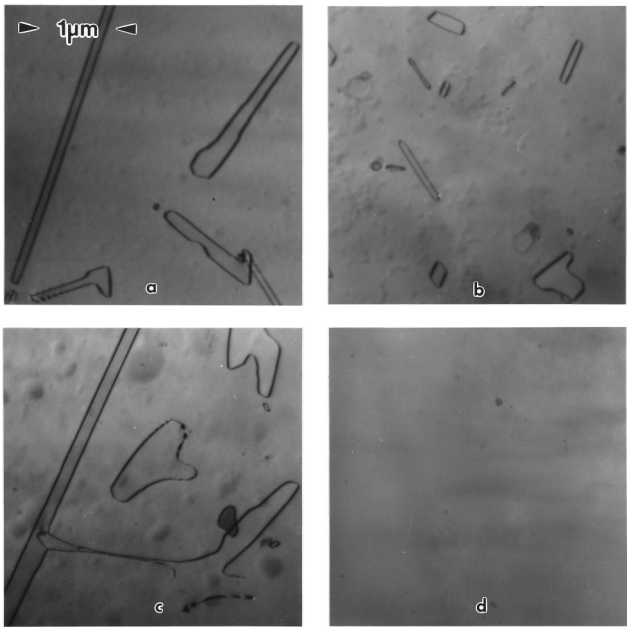

FIG. 1. Plan-view TEM images of the projected range dislocation loops after 1 MeVB^+ $1\times10^{14}/cm^2$ implant and annealing at (a) 1000 °C 30 s RTA, (b) 1100 °C 30 s RTA, (c) 1000 °C 60 min furnace annealing, (d) 1100 °C 60 min furnace annealing.

sity, the dislocations at the projected range, and the total concentration of interstitials bound by the dislocation loops at the projected range vary with RTA temperature for 30 s anneals. The methodology to determine the trapped interstitial concentration was discussed elsewhere[18] and has been combined with standard stereology methods. It is clear from Fig. 2 that the total concentration of interstitials after RTA annealing is remaining relatively fixed. The concentration of interstitials is approximately equal to the dose. This has been observed before for lower energy boron implants and to a first order is attributed injection of an extra atom by the implant[19,20] Figure 2 also shows that as one increases the RTA temperature the density of extended defects increases. Since the concentration of interstitials is remaining constant for the short anneal time, this increase in density translates into a decrease in the average diameter of the dislocation

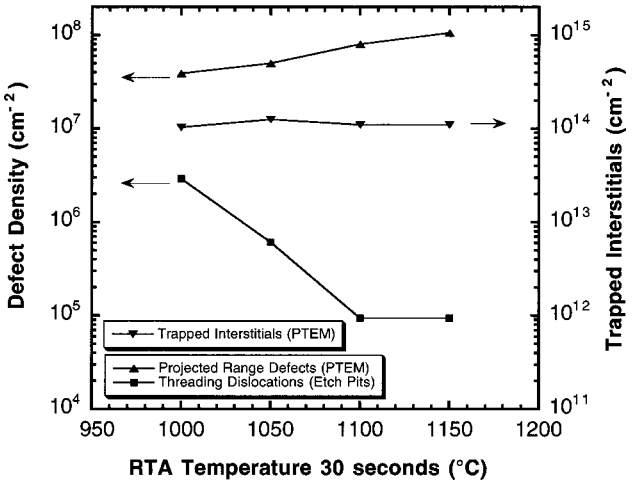

FIG. 2. Effect of RTA temperature on the threading dislocation density, projected range dislocation density, and the trapped interstitial density of a 1 MeVB^+ $1\times10^{14}/cm^2$ implant after annealing for 30 s.

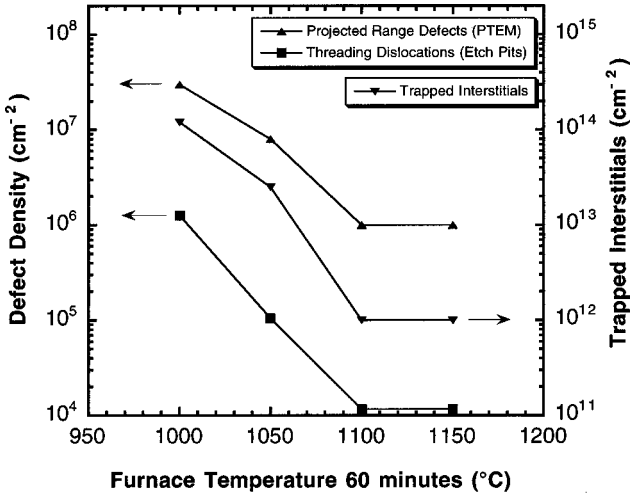

FIG. 3. Effect of furnace temperature on the threading dislocation density, projected range dislocation density, and the trapped interstitial density of a 1 MeVB^+ $1\times10^{14}/cm^2$ implant after annealing for 60 min.

loops. This is also visible in Fig. 1. It is also apparent from Fig. 2 that the threading dislocation density is decreasing dramatically between 1000 and 1100 °C. The value seems to stop decreasing at a density of around $1\times10^5/cm^2$. This decrease appears to correlate to the decrease in the dislocation loop diameter. The simple explanation for the decrease in threading dislocations is that, as the diameter of projected range dislocation decreases, fewer of these defects reach the surface and form threading dislocations. It remains unclear why higher temperatures would favor more numerous smaller dislocation loops. Clearly, during the anneal less time is spent at lower temperatures where large {311} defects can form. The dislocation loop formation process has been associated with unfaulting of the {311} defect and thus more numerous, smaller {311} defects might translate into more numerous smaller dislocation loops.[21,22]

Figure 3 shows the effect of 60 min isochronal annealing in the furnace on the threading dislocation density, the projected range dislocation loops, and the trapped interstitials in the projected range dislocations. Unlike the RTA anneals, the furnace anneals result in a significant decrease in the dislocation loop density with increasing annealing temperature. In addition, the trapped interstitial concentration in the defects is decreasing. The projected range dislocation density detection limit is $1\times10^6/cm^2$ and the trapped interstitial detection limit is about $1\times10^{12}/cm^2$. Figure 3 shows that by 1100 °C both of these densities drop below the detection limit. This translates into a marked decrease in the threading dislocation density as is apparent in Fig. 3. In this case the threading dislocation density drops below the etch-pit detection limit ($\sim1\times10^4/cm^2$) by 1100 °C.

It appears that for both the RTA anneal and the furnace anneal, 1100 °C is a critical temperature. However, the mechanism for the reduction in threading dislocation density appears to be different. In order to further explore this effect, 1100 °C isothermal anneals were carried out for times between 1 s and 1 h. Figure 4 is a plot of both the density of threading dislocations from etch-pit measurements and projected range dislocations from plan-view TEM measurements as a function of 1100 °C annealing time. It can be seen

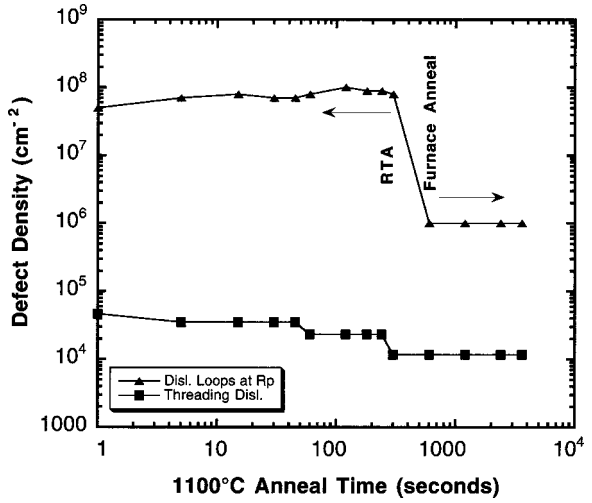

FIG. 4. Effect of annealing time on the threading dislocation density and projected range dislocation density of a 1 MeV B^+ $1\times10^{14}/cm^2$ implant after annealing at 1100 °C.

from the figure that the threading dislocation density shows a gradual decrease with increasing annealing time, however even the shortest time has already decreased the density by over an order of magnitude from the values at lower RTA temperatures seen in Fig. 2. It is also clear that the density of dislocation loops in the projected range after any 1100 °C RTA is fairly high and thus the mechanism discussed for Fig. 2 appears to apply for all RTA times studied. The RTA anneal times were carried out up to 5 min and the shortest furnace annealing time was 10 min. For furnace annealing times the mechanism appears to switch to one of complete dissolution of all damage since both the dislocation density and the threading dislocation density are below the detection limit. Thus the furnace annealing mechanism appears to hold for all furnace annealing times studied at 1100 °C.

The difference between the furnace and RTA anneals could have several sources. First, the calibration of the furnace and the RTA could be off. In order to calibrate the RTA an external thermocouple, which has been attached to a silicon wafer, was placed inside the processing chamber. The temperature from the thermocouple wafer was compared to that of the optical pyrometer and appropriate software compensation was made to ensure that the two temperatures measurements match each other. Similarly, a furnace was calibrated by placing a series of thermocouples into the processing chamber. The temperature from the thermocouples was compared to those of the furnace readout and appropriate software compensation was made to ensure that the two temperature measurements match each other.

The second possibility is that the ramp rate is important. As stated in the experimental description, the furnace annealing ramp rate was only 10 °C/s but the RTA ramp rate was 50 °C/s. Hamada, Nishio, and Saito[23] studied 1 MeV phosphorus implants, not boron implants, and observed that for 30 s anneals, higher ramp rates resulted in fewer threading dislocations compared to lower ramp rate annealing. No comparison to long time furnace anneals was done. This supports the concept that ramp rate is important in the nucleation of projected range dislocations and threading dislocations and further experiments are needed to determine the role of ramp rate for B^+ implants over a range of annealing conditions.

In conclusion, it has been shown that both RTA and furnace annealing at 1100 °C can result in a significant decrease in the density of threading dislocations. The mechanism by which the threading dislocation density decreases appears to depend on the annealing process. For the RTA process, increasing the temperature decreases the average size of the projected range dislocation loops which results in fewer threading dislocations. For the furnace annealing process, annealing at 1100 °C results in complete dissolution of the projected range dislocations and the threading dislocations. The time study at 1100 °C suggests that the difference between the RTA and furnace anneals does not appear to be directly related to the duration of the annealing but rather may be the result of the difference in the ramp rate of the annealing.

The authors would like to acknowledge the assistance of Erica Heitman and Josh Glassberg with the TEM sample preparation and Britta Jones/WW with some of the etch pit counts.

[1] H. Wong, N. W. Cheung, P. K. Chu, J. Liu, and J. W. Mayer, Appl. Phys. Lett. **52**, 1023 (1988).
[2] T. Kuroi, S. Komori, H. Miyatake, and K. Tsukamoto, Tech. Dig. Int. Electron Devices Meet., 261 (1990).
[3] D. C. Jacobson, A. Kamgar, D. J. Eaglesham, E. J. Lloyd, S. J. Hillenius, and J. M. Poate, Nucl. Instrum. Methods Phys. Res. B **96**, 416 (1995).
[4] L. M. Rubin, R. B. Simonton, S. D. Wilson, and W. Morris, Ion Implantation Technology-96, IEEE, 1997, Vol. TH8182, p. 13.
[5] R. A. Brown, O. Kononshuk, G. A. Rozgonyi, S. Koveshnikov, A. P. Knights, P. J. Simpson, and F. Gonzalez, J. Appl. Phys. **84**, 2459 (1998).
[6] M. Tamura, N. Natsuaki, Y. Wada, and E. Mitani, J. Appl. Phys. **59**, 3417 (1986).
[7] M. Tamura, N. Natsuaki, Y. Wada, and E. Mitani, Nucl. Instrum. Methods Phys. Res. B **21**, 438 (1987).
[8] W. Skorupa, E. Weiser, R. Groetzschel, M. Posselt, H. Buecke, A. Armigliato, A. Garulli, A. Beyer, and W. Markgraf, Nucl. Instrum. Methods Phys. Res. B **19/20**, 335 (1987).
[9] R. J. Schreutelkamp, J. S. Custer, J. R. Liefting, W. X. Lu, and F. W. Saris, Mater. Sci. Rep. **6**, 275 (1991).
[10] R. J. Schreutelkamp, J. S. Custer, J. R. Liefting, F. W. Saris, W. X. Lu, B. X. Zhang, and Z. L. Wang, Nucl. Instrum. Methods Phys. Res. B **62**, 372 (1992).
[11] J. Y. Cheng, D. J. Eaglesham, D. C. Jacobson, P. A. Stolk, J. L. Benton, and J. M. Poate, J. Appl. Phys. **80**, 2105 (1996).
[12] H. Sayama, M. Takai, Y. Akasaka, K. Tsukamoto, and S. Namba, J. Appl. Phys. **28**, 1673 (1989).
[13] M. Takahashi, S. Konaka, and K. Kajiyama, J. Appl. Phys. **54**, 6041 (1983).
[14] Y. T. Jang, T.-H. Huh, and J.-S. Ro, Ion Implantation Technology-98, IEEE, 1998, Vol. EX144, p. 959.
[15] C. Jasper, A. Hoover, and K. S. Jones, Appl. Phys. Lett. **75**, 2629 (1999).
[16] K. K. Bourdelle, D. J. Eaglesham, D. C. Jacobson, and J. M. Poate, J. Appl. Phys. **86**, 1221 (1999).
[17] D. G. Schimmel, J. Electrochem. Soc. **126**, 479 (1979).
[18] K. S. Jones, K. Moller, J. Chen, M. Puga-Lambers, B. Freer, J. Berstein, and L. Rubin, J. Appl. Phys. **81**, 6051 (1997).
[19] K. S. Jones, S. Prussin, and E. R. Weber, Appl. Phys. A: Solids Surf. **45**, 1 (1988).
[20] M. D. Giles, J. Electrochem. Soc. **138**, 1160 (1991).
[21] D. Eaglesham, P. Stolk, J.-Y. Cheng, H.-J. Gossmann, T. Haynes, and J. Poate, in Microscopy Semiconductor Mater. Conference Oxford, 1995, p. 451.
[22] J. Li and K. S. Jones, Appl. Phys. Lett. **73**, 3748 (1998).
[23] K. Hamada, N. Nishio, and S. Saito, Mater. Res. Soc. Symp. Proc. **396**, 739 (1996).